COVID-19 spreading and vaccine information diffusion interplay on age-based networks

Matteo Bortoletto,* Clelia Corridori,† and Michele Puppin‡

(Dated: January 16, 2021)

In the context of COVID-19 pandemic, vaccines seem to be the best option for slowing down disease spreading. In this work, we want to understand the role of vaccine information spreading withing this framework. To do that, we start from a model that describes a SIR-SIRV dynamics for information and disease transmission on a multiplex network. As result, we find that there exists an optimal information transmission rate that slows down the spreading of the disease, increasing the number of individuals that get vaccinated. Then, we implement a variation of this model that takes into account demographic and epidemiological features relevant for COVID-19 disease. It consists in a SIR-SIARV age-based model that considers two age groups of individuals and the role of asymptomatic individuals. For this new model, we find again the existence of an optimal information transmission rate. This result can be employed in policy making, to tune the information diffusion to get the higher possible number of immunized individuals.

I. INTRODUCTION

The 21th December 2020 the European Commission authorised the first vaccine to prevent COVID-19 in the European Union, following the evaluation by the European Medicine Agency [4]. This event represents an important turning point that will change the evolution of the world dynamics. Due to the absence of pharmaceutical interventions against COVID-19, deep upheaval has occurred in the last year: social norms have changed, lockdowns, quarantine and other preventive measures have been introduced and people have adopted a new lifestyle. Now, vaccines offer the possibility to slow down COVID-19 spreading and it is important to understand how their introduction and how vaccine information spreading will change the dynamics.

The interplay of these two factors can lead to nontrivial phenomena thanks to the fact that their dynamics are not independent [14]. Indeed, by looking at the link between biological and social spreading we know that there are different tendencies that correlate the two dynamics. For example, people who are aware of the effects of disease spreading tend to protect themselves, whereas misinformation can change the perception of the danger of infection, decreasing the level of vaccinated people. Moreover, high levels of vaccine coverage can decrease disease incidence, reducing the perceived danger [11] [5]. Therefore, understanding the coevolution of disease and information spreading is important to develop methods to predict and control COVID-19 disease spreading by using vaccines and awareness campaigns.

In this work we start from the model implemented by W. Wang and his collaborators [14], describing with multiplex network the information and disease transmission topologies. We adjust it to study COVID-19 spreading, in particular for Italy. To do that, two uncorrelated networks are considered: the communication layer (A) and the contact layer (B), each one with its specific degree distribution $P_A(k_A)$ and $P_B(k_B)$, respectively. For each layer, nodes represent individuals and edges are contacts among individuals; each node in A corresponds to a node in B. We will inspect both random networks and scale-free networks as types of network for our model.

To describe the dynamics on the two layers we use compartmental models, labelling each node with its compartment at each time step and using transitions mediated by rates to capture the population-level dynamics from the microscopic contagion process. For the communication layer we use a Susceptible-Infected-Recovered (SIR) epidemiological model, assuming that infected (or informed) individuals are aware of the disease and participate to information spreading, while recovered are aware but do not communicate their knowledge. For the contact layer we start by considering a Susceptible-Infected-Recovered-Vaccinated (SIRV) model, assuming that people can not be reinfected in the considered time interval.

In this model we include an asymmetric interaction between information and disease dynamics. In fact, real-world data analysis reveals that, while disease spreading promotes the information spreading, information spreading suppresses disease spreading [14]. On the communication layer, information outbreak can be triggered by its own spreading dynamics or by the disease outbreak in the contact network. On the other hand, the disease threshold is not affected by information spreading. Furthermore, there is an optimal information transmission rate that suppresses the disease spreading [14]. This result could be employed to plan vaccination information campaigns for COVID-19.

Thus, as further analysis, we implement a variation of the model that takes into account demographic and epidemiological features which are relevant for COVID-19 disease. In particular, an age-based model that considers two age groups of individuals is presented, indeed the number of contacts is correlated to age [9]. These features are taken into account by defining an age-based

* matteo.bortoletto.2@studenti.unipd.it
† clelia.corridori@studenti.unipd.it
‡ michele.puppin@studenti.unipd.it

network, which we call CMM. Moreover, in COVID-19 spreading dynamics, the role of asymptomatic individuals has shown to be crucial [10] and the fraction of asymptomatic cases depends on age, as will be highlighted in Sec. II. For the communication layer we still use a SIR model. For the contact layer we use a Susceptible-Infected-Asymptomatic-Recovered-Vaccinated (SIARV) model, where A denotes the presence of asymptomatic infectious. Our aim is to study how the coevolution dynamics changes if we consider the differences between the two age groups. Again, the purpose is to search a strategy to make vaccine diffusion as large as possible.

II. METHODS

A. SIR-SIRV dynamics

In order to analyze how the diffusion of vaccine information can affect COVID-19 spreading, we consider a model composed of two layers. In the communication layer (A) we implement a SIR model to reproduce the dynamics of information diffusion, where we consider an informed individual as infected. In the contact layer (B) we use a SIRV model for the disease spreading. In particular, a vaccinated individual behaves exactly as a recovered individual. The dynamics occur on two networks, one for each layer, and each node in layer A is randomly matched one-to-one with a node in layer B. The correspondence between the two layers allows to model the asymmetrical interaction between information diffusion and disease spreading. The dynamics on the two layers evolve as follows.

SIR In layer A, a susceptible node (S_A) becomes informed with probability β_A if it has an infected neighbour, while an infected node (I_A) will become recovered (R_A) with probability γ_A. Moreover, a susceptible node automatically becomes informed (I_A) if its counterpart in layer B is infected (I_B).

SIRV In layer B, a susceptible node (S_B) becomes infected with probability β_B if it has an infected neighbour, while an infected node (I_B) will become recovered (R_B) with probability γ_B. A susceptible node can become vaccinated (V_B) with probability p if two conditions occur simultaneously: *(i)* its counterpart in layer A is informed (I_A) and *(ii)* at least a number φ of neighbours, which we call immunization threshold, in layer B are infected (I_B).

The two networks are randomly generated and uncorrelated. First of all, we implement an algorithm to generate an Erdős-Rényi graph (ER) for modelling the communication and contact networks. Moreover, we implement an algortihm to generate a Barabási-Albert graph in order to consider also scale free networks (SF).

We apply the model to COVID-19 spreading. Recent studies show that COVID-19 infection produce a good level of immunity, lasting at least several months [13]. Therefore, given the time window considered in our analysis, the assumption of a SIRV compartmental model for the disease is reasonable. We set COVID-19 infectious period to $\tau_B = 5$ days [6], and we compute the recovery rate $\gamma_B = 1/\tau_B$. We consider a basic reproductive number $R_0 \approx 3$ [7] and in our analysis we always choose a set of transmission rates β_B around the value that reproduces the chosen R_0. The probability of vaccination is set to $p = 0.8$ and the number of infected neighbours needed for the vaccination varies in a set of values $\varphi = 1, 3, 5$ [14]. For the information layer we choose the same values of transmission and recovery rate [14]. We consider two networks with average number of contacts $\langle k_A \rangle = \langle k_B \rangle = 8$ [14].

B. SIR-SIARV age-based dynamics

The role of asymptomatic individuals has shown to be crucial in the diffusion of COVID-19 [10]. Therefore, we introduce the symptomatic and asymptomatic state for diseased individuals (SIARV) in layer B. Moreover, in order to consider the impact of individuals' age on information diffusion and epidemic spreading, we design an age-based model, based on the previous model. According to their age, individuals are divided in two classes that behave differently. We also take into account the fact that the proportion of asymptomatic cases varies in different age groups. The mixing inside different age groups varies as well; younger individuals are characterized by a higher contact rate while older individuals usually have a lower contact rate [9].

The dynamics of the two layers is analogous to the previous model, with the following variations.

SIR In layer A, a susceptible node (S_A) becomes infected with probability $r\beta_A$ if it has an infected neighbour, where r is a reduction factor. Indeed, we assume that increasing the age, people are less likely to be informed so the information rate is reduced. We choose to set $r = 1$ for younger individuals and $r = 0.8$ for older ones, as hypothetical representative value. Moreover, a susceptible node automatically becomes informed (I_A) if its counterpart in layer B is symptomatic infected (IS_B).

SIARV In layer B, a susceptible (S_B) node becomes infected with probability β_B if it has an infected neighbour; infected nodes can be asymptomatic (IA_B) with probability p_{asym} or symptomatic (IS_B) with probability $1 - p_{asym}$. We assume symptomatic and asymptomatic infected nodes to behave identically as far as infection and recovery processes are concerned. A susceptible node can become vaccinated (V_B) with probability p if two conditions occurs simultaneously: *(i)* its counterpart in layer A is informed (I_A) and *(ii)* at least a number φ of neighbours in layer B are symptomatic infected (IS_B).

We implement an algorithm to generate an age-based network. An empty graph is created and nodes are labeled as *young* (Y) or *old* (O) in a predefined fraction. Edges are added as follows: a node Y has a probability p_{YY} to link with another node Y and probability p_{YO}

Age	0-9	10-19	20-29	30-39	40-49	50-59	60-69	70-79	80-89	>90
f	0.77	0.71	0.66	0.63	0.61	0.60	0.59	0.56	0.57	0.65

TABLE I. Fraction of asymptomatic cases over total number of cases with ongoing disease f, differentiated for most recent symptomatology and for age group [1].

to link with a node O; a node O has a probability p_{OO} to link with another node O and probability p_{YO} to link with a node Y. The two networks are again randomly generated and uncorrelated.

We analyze real data on COVID-19 disease and demography to set the model parameters accordingly. Firstly, we consider the incidence of asymptomatic cases based on the age group. In Tab. I we show the data regarding the fraction of asymptomatic cases in Italy [1]. We choose 0-49 age group as *young* (Y) and above 50 age group as *old* (O). In fact, the age of 50 seems to be a turning point both for contact rates [8][9] and disease severity for COVID-19 [8][12]. To set the probabilities of being asymptomatic, we consider the average fraction of asymptomatic cases for each age group: $p_{asym,Y} = 0.68$ for *young* individuals and $p_{asym,O} = 0.59$ for *old* individuals. To build the CMM network, we set the number of nodes to $N_A = N_B = 10^4$ and the fraction of *young* nodes to 0.55, based on Italy demographic data [2]. Nodes in layer A are randomly linked to nodes belonging to the same age group in layer B. Finally, we set the probabilities p_{YY}, p_{OO} and p_{YO} to values that reproduce realistic surveyed number of links for each age group. The total average number of contacts per day are $\langle k_Y \rangle \approx 22$ for *young* individuals and $\langle k_O \rangle \approx 12$ for *old* individuals. The 57% of contacts are found to be between *young* people, 21% between *old* people and 22% are contacts between the two age groups [3]. The values of transmission rate and recovery rate for both layers are the same as the ones considered for the previous model.

III. RESULTS

We perform extensive stochastic simulations to study the proposed dynamics on multiplex networks. The network sizes are set to $N_A = N_B = 10^4$. For each multiplex network, we perform the dynamics for 100 time-steps, each one corresponding to one day, for 100 times. We measure the average final fraction of information size R_A, disease size R_B, and vaccination size V_B with 10 randomly selected seeds in layer B. We then average these results over 10 network realizations for the SIR-SIRV model and over 40 network realizations for the SIR-SIARV age-based model. The simulation code, together with the complete set of figures, is available on GitHub.

A. SIR-SIRV dynamics

For the SIR-SIRV dynamics we use ER graphs both for communication and contact networks. Contact probabilities are set to $p_A = p_B = 8 \cdot 10^{-4}$ so that the average degrees obtained are $\langle k_A \rangle \approx 8$ and $\langle k_B \rangle \approx 8$.

Fig. 1 shows how the immunization threshold φ affects the final information, disease, and vaccination sizes. Notice that R_A increases with β_A and β_B [Fig. 1(a,d)], as we expect. So, we can say that information spreading increases as disease spreading increases. Moreover, R_A increases also with φ. This is due to the fact that for individuals in layer B it is more difficult to decide to get vaccinated if φ is large [Fig. 1(c,f)]. As a consequence, more individuals will become informed because of getting the disease. In fact, R_B increases with φ [Fig. 1(b,e)], while V_B decreases with φ [Fig. 1(c,f)]. Note that V_B (R_B) has a non-monotonic shape, in fact it first increases (decreases) with β_A and then decreases (increases). Thus, they have a minimum which represents an optimal information transmission rate β_A^*. Qualitatively, we can give an explanation of this behaviour recalling that a node on layer B is vaccinated only when its counterpart in layer A is informed and when the number of its infected neighbours is larger than φ. For small values of β_A, the first condition is hard to satisfy, because information spreads very slowly. Conversely, for large values of β_A the second condition is never satisfied because information spreads too quickly. This causes V_B to decrease with β_A and the spreading of the disease is enhanced. Fig. 1(e) shows that the disease epidemic threshold $\beta_{B,c}$ for $\varphi = 1$ is larger than the one for $\varphi = 3, 5$. Clearly, this happens because if we introduce an immunization threshold an individual is vaccinated only when the number of its infected neighbours is above it.

Fig. 2 shows the final information, disease, and vaccination sizes for $\varphi = 3$. By looking at Fig. 2(a) we can see that, for all the three values of β_B, any value of β_A can cause an outbreak of the information, meaning that the information epidemic threshold is $\beta_{A,c} = 0$. Fig. 2(b,c) show again the optimal information transmission rate for which R_B (V_B) is minimum (maximum). Fig. 2(d) shows that, for all the three values of β_A, R_A increases with β_B because by increasing the disease spreading we get more informed nodes. Fig. 2(e) shows that β_A does not affect the disease epidemic threshold $\beta_{B,c}$.

Fig. 3 shows the macroscopic coevolution of the two dynamics under different information transmission rates, for $\varphi = 3$. In particular, we consider three values of β_A: the first below β_A^*, the second equal to β_A^* and the third above β_A^*. To study the relationship between information spreading and disease spreading we separately consider the fraction of nodes on layer A informed by their neighbours $\rho_A^A(t)$ or by their counterparts of layer B $\rho_A^B(t)$. Then, $\rho_B(t)$ represents the fraction of infected nodes of layer B at time t. Fig. 3(a) shows that, for $\beta_A < \beta_A^*$, ρ_A^A, ρ_A^B and ρ_B reach their peaks simultaneously. Furthermore, notice that ρ_B is larger than ρ_A^A and very close to

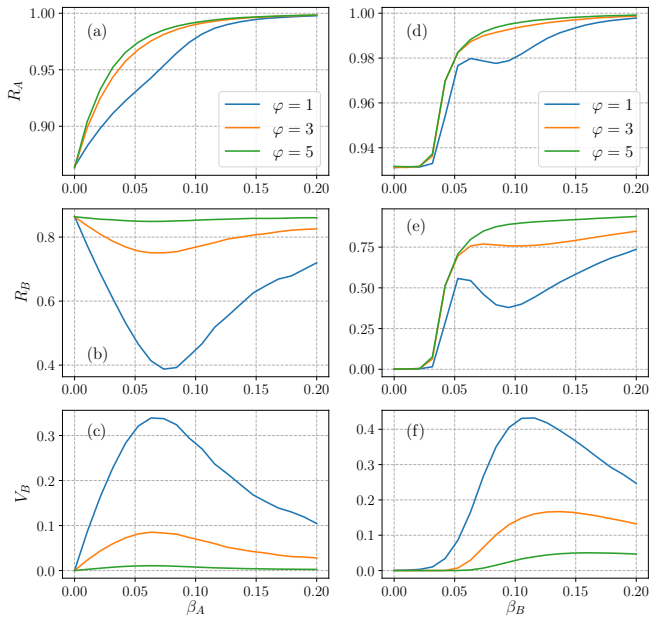

FIG. 1. Final sizes of information, disease and vaccination on two ER-ER layers for different values of φ. (a) The final information size R_A, (b) the final disease size R_B, and (c) the final vaccination size V_B versus information transmission rate β_A, with $\beta_B = 0.075$. (d) R_A, (e) R_B and (f) V_B as a function of β_B at $\beta_A = 0.1$. The probability of getting vaccinated is set to $p = 0.8$.

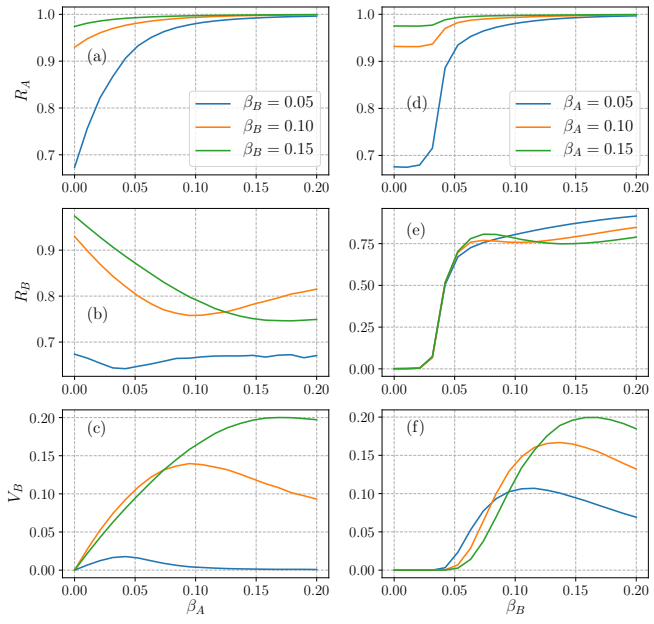

FIG. 2. Final sizes of information, disease and vaccination on two ER-ER layers, for different values of β_A and β_B. (a) The final information size R_A, (b) the final disease size R_B, and (c) the vaccination size V_B versus the information transmission rate β_A, for $\beta_B = 0.05$, 0.10 and 0.15. For $\beta_A = 0.05$, 0.10 and 0.15, (d) R_A, (e) R_B and (f) V_B as a function of β_B. Other parameters are $\varphi = 3$ and $p = 0.8$.

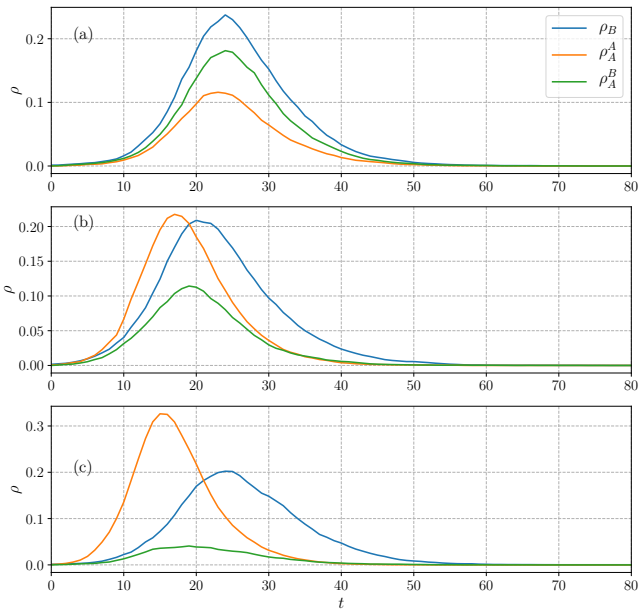

FIG. 3. On ER-ER coupled networks, the time evolution of $\rho_A^A(t)$, $\rho_A^B(t)$ and $\rho_B(t)$ for (a) $\beta_A = 0.033$, (b) $\beta_A = 0.063$ and (c) $\beta_A = 0.093$. Other parameters are set to be $\beta_B = 0.075$, $\varphi = 3$ and $p = 0.8$.

ρ_A^B, meaning that the spread of information is primarily induced by the disease outbreak. Fig. 3(b) shows that, for $\beta_A = \beta_A^*$, ρ_B is closer to ρ_A^A than to ρ_A^B. So, at the optimal information transmission rate, information and disease have a similar macroscopic coevolution. Fig. 3(c) shows that for $\beta_A > \beta_A^*$ information spreads more quickly than the disease.

Finally, to verify the dependency of these results on the chosen network, we test our dynamics on SF-SF multiplex networks, obtaining analogous behaviours.

B. SIR-SIARV age-based dynamics

For the SIR-SIARV dynamics we use CMM graphs with probabilities $p_{YY} = 1.6 \cdot 10^{-3}$, $p_{OO} = 8.9 \cdot 10^{-4}$ and $p_{YO} = 3.8 \cdot 10^{-4}$ both for communication and contact network. The resulting average degree for the two age groups are $\langle k_Y \rangle \approx 22$ and $\langle k_O \rangle \approx 12$ for both layers.

As we can see by looking at Fig. 4, Fig. 5 and Fig. 6, the results are quite similar for both age groups. Probably this happens because there are some parameters, estimated by analyzing real world data, that do not differ significantly between the two groups. This aspect will be better discussed in Sec. IV. That said, we will proceed by comparison with the SIR-SIRV dynamics considering only one of the two groups, namely the *young*.

Fig. 4(Y)(a,d) show that R_A increases with β_A and β_B, as we expect. Apparently, now R_A seems not to increase with φ. This may suggest that the contribution to information dynamics of individuals who become in-

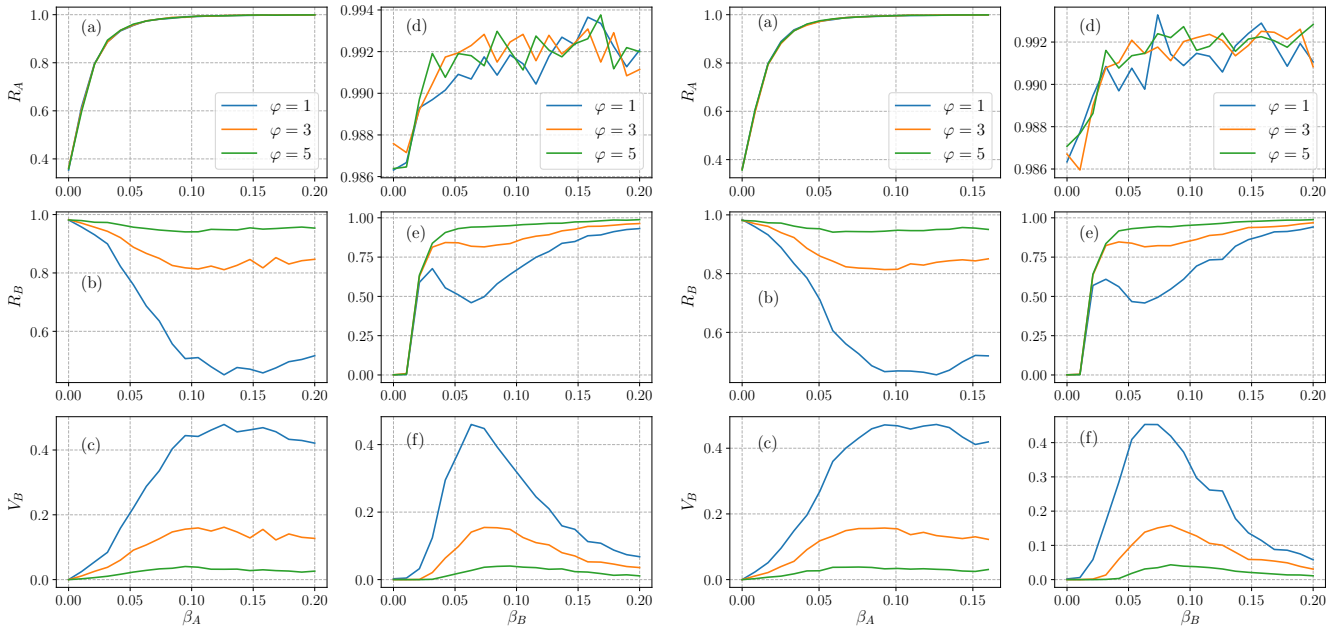

(Y) Young. (O) Old.

FIG. 4. Final sizes of information, disease and vaccination on two CMM-CMM layers for different values of φ. (a) The final information size R_A, (b) the final disease size R_B, and (c) the final vaccination size V_B versus information transmission rate β_A, with $\beta_B = 0.075$. (d) R_A, (e) R_B and (f) V_B as a function of β_B at $\beta_A = 0.1$. The probability of getting vaccinated is set to $p = 0.8$. In (O), we plot the reduced β_A, i.e. $r\beta_A$.

formed because of getting the disease is smaller than the one of information diffusion. Fig. 4(Y)(d) shows a flattening of the curves. In particular, for small values of β_B, R_A is larger than the one in Fig. 1(d), because information spreads faster due to the chosen higher degree of the communication network. Again, Fig. 4(Y)(b,e) show that R_B increases with φ. This happens because V_B decreases with φ [Fig. 4(Y)(c,f)]. In fact, for higher values of φ it is more difficult to decide to get vaccinated. Note that R_B (V_B) still have a minimum (maximum), which represents the optimal information transmission rate β_A^*. Moreover, Fig. 4(Y)(e) shows that the disease epidemic threshold $\beta_{B,c}$ is equal for all values of φ and lower than the one for SIR-SIRV dynamics. Fig. 5(Y) shows the final information, disease, and vaccination sizes for $\varphi = 3$. By looking at Fig. 5(Y)(a) we can see that the information epidemic threshold is again $\beta_{A,c} = 0$. Note that the three curves collapse, meaning that information spreading is not influenced by the transmission rate of the disease. This is confirmed by looking at Fig. 5(Y)(d), where we observe flat lines. In fact, because of the presence of asymptomatic individuals, it is more difficult to become informed by getting the disease. Fig. 5(Y)(b,c,f) show a behaviour which is analogous to the one observed in Fig. 2(b,c,f). Fig. 5(Y)(e) shows that β_A does not affect the disease epidemic threshold $\beta_{B,c}$, which now is lower.

Fig. 6 shows the macroscopic coevolution of the two dynamics under different information transmission rates. As before, we consider three values of β_A: the first below β_A^*, the second equal to β_A^* and the third above β_A^*. Fig. 6(a,b,c) show that, for any value of β_A, ρ_A^A is always larger than ρ_A^B, meaning that the disease spreading is not the primary cause of information spreading. Moreover, Fig. 6(b,c) show that by increasing the value of β_A the disease outbreak does not play any role in the process of information spreading. Fig. 6(d,e,f) show that for *old* individuals the fraction of individuals becoming informed because of getting the disease is larger with respect to *young* individuals. This is due to the fact that *old* individuals are characterized by a higher fraction of symptomatic cases and lower information transmission rate. However, it is still marginal with respect to ρ_A^A.

IV. DISCUSSION AND CONCLUSIONS

In the first part of this work, by assuming an asymmetrical interaction between information and disease dynamics, we find that there exists an optimal information transmission rate that slows down the spreading of the disease, increasing the number of individuals that get vaccinated. Then, we consider a model which is more suited to describe the current COVID-19 pandemics. On the epidemiological side, we take into account specific characteristics of COVID-19, such as the large fraction of asymptomatics. On the demographic side, we consider two different age groups with different average number of

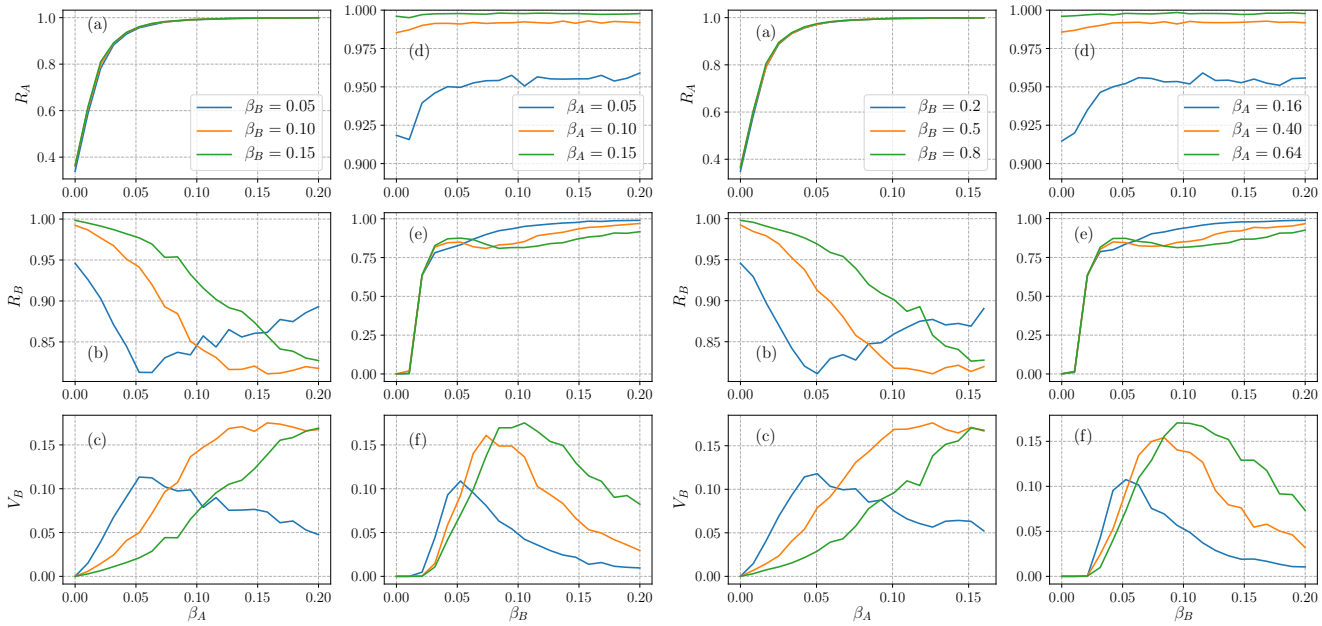

FIG. 5. Final sizes of information, disease and vaccination on two CMM-CMM layers, for different values of β_A and β_B. (a) The final information size R_A, (b) the final disease size R_B, and (c) the vaccination size V_B versus the information transmission rate β_A for the disease transmission rate $\beta_B = 0.05$, 0.10 and 0.15. For $\beta_A = 0.05$, 0.10 and 0.15, (d) R_A, (e) R_B and (f) V_B as a function of β_B. Other parameters are $\varphi = 3$ and $p = 0.8$. In (O), we plot the reduced β_A, i.e. $r\beta_A$.

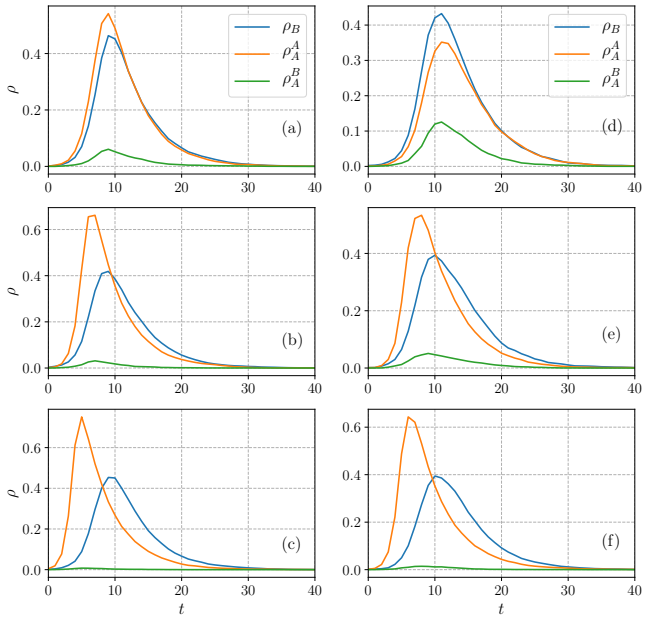

FIG. 6. For the two age groups *young* (a,b,c) and *old* (d,e,f), on CMM-CMM coupled networks, the time evolution of each type of nodes. The time evolution of $\rho_A(t)$, $\rho_A^A(t)$, $\rho_A^B(t)$ and $\rho_B(t)$ for (a) $\beta_A = 0.076$, (b) $\beta_A = 0.126$, (c) $\beta_A = 0.176$, (d) $\beta_A = 0.066$, (e) $\beta_A = 0.116$ and (f) $\beta_A = 0.166$. Other parameters are set to be $\beta_B = 0.075$, $\varphi = 3$ and $p = 0.8$.

contacts, information transmission rate and incidence of symptoms. Again, we find the emergence of an optimal information transmission rate, which is larger than the one obtained before. This result is found for both age groups, in particular the optimal value results to be slightly higher for *young* individuals. By running the SIR-SIRV dynamics on a ER-ER network with similar mean degrees to the ones of the considered CMM-CMM network, we compare the final fraction of vaccinated individuals. With the SIR-SIARV age-based model we observe a smaller fraction of vaccinated individuals, due to the presence of asymptomatic individuals. Moreover, in the SIR-SIARV age-based model the fraction of individuals that become informed because of getting the disease is reduced, again by the presence of asymptomatic individuals. As already highlighted, we observe no significant differences between the dynamics of the two age groups. Several explanations are possible. First of all, the chosen age threshold, which represents the turning point both for contact rates and disease severity for COVID-19, leads to a similar occupancy of the two age groups. Then, despite the different average number of contacts for the two age groups, considering that the probability of connection between the two age group is not negligible, we find that the two communities are well connected. Moreover, the fraction of asymptomatic individuals does not differ significantly for the two age groups. Eventually, the reduction in information transmission rate considered for *old* individuals appears not to be noteworthy. Other

values could be inspected.

We now consider the limitations of our model. First of all, the assumption of SIRV and SIARV dynamics for the spreading of COVID-19 disease is reasonable as long as we consider a suitable time interval. In fact, further studies may show a waning immunity induced both by the disease and the vaccine. Furthermore, the assumption of a SIR dynamics for information diffusion may not hold in the peculiar frame of a global pandemic which heavily affects individuals' life. In particular, the assumption that recovered individuals in communication layer do not vaccinate is aimed to focus on the fact that we are interested on how people react when they see a certain number of infected individuals near them. Another limitation of our model is that we assume information to spread only by means of face to face human interaction. That is, we do not consider the presence of social networks, which in truth is quite predominant nowadays. Finally, for sake of simplicity, we consider only two age groups. This choice leads to compute averages over different individuals which are, in principle, quite different but that fall into the same group. Other values for the age threshold and different number of age groups could be inspected. Many parameters have been introduced in SIR-SIARV age-based model. Therefore, further analysis may help to explore how each one influences the dynamics. Moreover, different behaviours between symptomatic and asymptomatic individuals (i.e. different transmission rates or different number of contacts) could be considered to build a more realistic model.

The results obtained for the SIR-SIARV age-based model highlight that, while age seems to be not relevant for information diffusion, special attention should be paid to the role of asymptomatic individuals, which represent an obstacle to disease awareness. Nevertheless, the fact that our model shows the existence of an optimal information transmission rate can be employed in policy making, to tune information diffusion accordingly to the percentage of asymptomatic cases. In this way, it may be possible to design efficient vaccination campaigns, which are more likely to get the higher possible number of immunized individuals.

REFERENCES

[1] *COVID-19 integrated surveillance data in Italy.* https://www.epicentro.iss.it/en/coronavirus/sars-cov-2-dashboard.

[2] *Population pyramids of the world from 1950 to 2100.* https://www.populationpyramid.net/italy/2019/.

[3] *Social contact rates data tool.* http://www.socialcontactdata.org/socrates/.

[4] *Union register of medicinal products for human use.* https://ec.europa.eu/health/documents/community-register/html/h1528.htm.

[5] C. T. Bauch and A. P. Galvani, *Social factors in epidemiology*, Science, 342 (2013), pp. 47–49.

[6] A. W. Byrne, D. McEvoy, A. B. Collins, K. Hunt, M. Casey, A. Barber, F. Butler, J. Griffin, E. A. Lane, C. McAloon, K. O'Brien, P. Wall, K. A. Walsh, and S. J. More, *Inferred duration of infectious period of SARS-CoV-2: rapid scoping review and analysis of available evidence for asymptomatic and symptomatic COVID-19 cases*, BMJ Open, 10 (2020).

[7] M. D'Arienzo and A. Coniglio, *Assessment of the SARS-CoV-2 basic reproduction number, R0, based on the early phase of COVID-19 outbreak in Italy*, Biosafety and Health, 2 (2020), pp. 57 – 59.

[8] N. G. Davies, P. Klepac, Y. Liu, K. Prem, M. Jit, C. A. B. Pearson, B. J. Quilty, A. J. Kucharski, H. Gibbs, S. Clifford, A. Gimma, K. van Zandvoort, J. D. Munday, C. Diamond, W. J. Edmunds, R. M. G. J. Houben, J. Hellewell, T. W. Russell, S. Abbott, S. Funk, N. I. Bosse, Y. F. Sun, S. Flasche, A. Rosello, C. I. Jarvis, R. M. Eggo, and C. C.-. working group, *Age-dependent effects in the transmission and control of COVID-19 epidemics*, Nature Medicine, 26 (2020), pp. 1205–1211.

[9] S. Del Valle, J. Hyman, H. Hethcote, and S. Eubank, *Mixing patterns between age groups in social networks*, Social Networks, 29 (2007), pp. 539–554.

[10] H. M. Dobrovolny, *Modeling the role of asymptomatics in infection spread with application to SARS-CoV-2*, PLOS ONE, 15 (2020), pp. 1–14.

[11] S. Funk, E. Gilad, C. Watkins, and V. A. A. Jansen, *The spread of awareness and its impact on epidemic outbreaks*, Proceedings of the National Academy of Sciences, 106 (2009), pp. 6872–6877.

[12] G. Onder, G. Rezza, and S. Brusaferro, *Case-fatality rate and characteristics of patients dying in relation to COVID-19 in Italy*, JAMA, 323 (2020).

[13] N. Sherina, A. Piralla, L. Du, H. Wan, M. Kumagai-Braesh, J. Andréll, S. Braesch-Andersen, I. Cassaniti, E. Percivalle, A. Sarasini, F. Bergami, R. Di Martino, M. Colaneri, M. Vecchia, M. Sambo, V. Zuccaro, R. Bruno, T. Oggionni, F. Meloni, H. Abolhassani, F. Bertoglio, M. Schubert, M. Byrne-Steele, J. Han, M. Hust, Y. Xue, L. Hammarström, F. Baldanti, H. Marcotte, and Q. Pan-Hammarström, *Persistence of SARS-CoV-2 specific B- and T-cell responses in convalescent COVID-19 patients 6-8 months after the infection*, bioRxiv, (2020).

[14] W. Wang, Q.-H. Liu, S.-M. Cai, M. Tang, L. A. Braunstein, and H. E. Stanley, *Suppressing disease spreading by using information diffusion on multiplex networks*, Scientific Reports, 6 (2016), p. 29259.